

# Cherenkov sound on a surface of a topological insulator

Sergey Smirnov

*Institut für Theoretische Physik, Universität Regensburg, D-93040 Regensburg, Germany*

(Dated: May 29, 2022)

Topological insulators are currently of considerable interest due to peculiar electronic properties originating from helical states on their surfaces. Here we demonstrate that the sound excited by helical particles on surfaces of topological insulators has several exotic properties fundamentally different from sound propagating in non-helical or even isotropic helical systems. Specifically, the sound may have strictly forward propagation absent for isotropic helical states. Its dependence on the anisotropy of the realistic surface-states is of distinguished behavior which may be used as an alternative experimental tool to measure the anisotropy strength. Fascinating from the fundamental point of view backward, or anomalous, Cherenkov sound is excited above the critical angle  $\pi/2$  when the anisotropy exceeds a critical value. Strikingly, at strong anisotropy the sound localizes into a few forward and backward beams propagating along specific directions.

PACS numbers: 73.20.At, 63.20.kd, 41.60.Bq, 43.35.+d

## I. INTRODUCTION

A topological insulator (TI)<sup>1,2</sup> is a system supporting helical states<sup>3,4</sup> at its edges. These states, characterized by strong coupling between their spin degree of freedom and direction of propagation, appear as Kramers pairs and have zero gap as a consequence of the  $T$ -invariance. At the same time the bulk states have a finite gap. Therefore, these systems represent a phase of matter with coexisting metallic edge and insulating bulk. Importantly, the helical states are necessarily edge states (one- or two-dimensional (2D)) of a bulk system (two- or three-dimensional (3D)) and do not exist in truly one-dimensional or 2D systems since the  $T$ -invariance requires for fermions an even number of Dirac points.

One-dimensional helical states have been experimentally implemented in semiconductor quantum wells<sup>5</sup> where the quantum spin Hall effect has been observed in the regime of the inverted band structure supporting dissipationless edge currents<sup>6</sup>.

Of particular interest for the present study are 3D TIs supporting 2D helical states<sup>7</sup>. These surface states have been experimentally observed, *e.g.*, in  $\text{Bi}_2\text{Te}_3$ <sup>8</sup>, where a single nondegenerate Dirac cone is located at the  $\Gamma$  point of the surface Brillouin zone. The isotropic conic dependence of the electron energy on the momentum inherent to low-energy states breaks at higher energies. Here cubic in momentum terms reduce the continuous rotational symmetry down to the discrete threefold rotational symmetry. As a result, the shape of constant energy contours becomes hexagonal<sup>9,10</sup> as observed in experiments<sup>8</sup>. This anisotropic energy-momentum dependence may lead to fundamentally new behavior of physical observables. In particular, in Ref. 11 it has been predicted that the dielectric function obtained within the random phase approximation may become anisotropic in the momentum space.

Here we address an alternative issue related to the existence of the helical states and explore their impact on other degrees of freedom, namely lattice vibrations, with

a special focus on the Cherenkov sound (CS) excited by helical particles on a surface of a 3D TI.

The Cherenkov effect<sup>12,13</sup> is a fundamental physical phenomenon having both optic<sup>14</sup> and acoustic<sup>15</sup> manifestations. In particular, in the acoustic Cherenkov effect a medium emits a forward sound, distributed within the Cherenkov cone, under the impact of an electron whose velocity is larger than the sound velocity of this medium. This situation may change when there appears a strong coupling between the orbital and spin electronic degrees of freedom. It has been shown in Ref. 16 that in a 2D system with the Rashba<sup>17</sup> spin-orbit interaction electrons can excite anomalous CS, which propagates outside the Cherenkov cone in forward and backward directions. Here anomalous CS appears in a homogeneous system due to interchiral transitions specific to spin-orbit coupled systems.

This outstanding property of the CS in systems with strong spin-orbit coupling provides a platform for new applications in acoustic amplification based currently mainly on the normal CS. These more conventional applications include, *e.g.*, acoustic amplification in confined systems such as Si/SiGe/Si heterostructures<sup>18</sup> or the Cherenkov emission in polar bulk semiconductors<sup>19</sup> such as GaAs.

It is important to mention that in optics an anomalous Cherenkov effect may appear in the absence of spin-orbit coupling but due to strong inhomogeneity of systems as has been achieved, *e.g.*, in photonic crystals<sup>20</sup>.

Turning to the CS on a surface of a 3D TI one might expect a picture similar to the one in a 2D Rashba gas. Indeed, as a result of a strong spin-orbit coupling, anomalous CS must appear due to interchiral transitions and propagate forward and backward. However, this scenario cannot be realized: since the velocity  $v$  on the Dirac cone is much larger than the sound velocity  $c$ ,  $v \gg c$ , interchiral transitions do not contribute and the CS is of pure intrachiral nature.

As has been demonstrated in Ref. 16, in this case there can be excited only normal CS with the standard

features: 1) the sound is located within the Cherenkov cone whose angle  $\phi_c$  is (because of  $v \gg c$ ) close to  $\pi/2$ ,  $\phi_c \approx \pi/2$ ; 2) its strictly forward propagation is forbidden.

Here we demonstrate that the discrete threefold rotational symmetry of the system drastically changes this standard picture and leads to fundamentally new features of the CS propagating on a surface of a TI. Among these features are 1) strictly forward propagation and its remarkable and valuable for experiments dependence on the anisotropy of the helical states; 2) anomalous propagation outside the Cherenkov cone, *i.e.*, for angles  $\phi > \phi_c$ ; 3) localization into a finite number of normal and anomalous beams in the regime of strong anisotropy.

These remarkable features of the CS distinguish TIs from other systems such as, *e.g.*, graphene. Indeed, the strictly forward sound is obviously absent in graphene because in this system the spinor components have the same absolute value while on a surface of a TI they have different absolute values (see the next section). In other words, what physically distinguishes the CS on a surface of a TI is the finite out-of-plane spin polarization of this surface. A recent investigation of the CS in graphene and its application to hypersonic devices may be found for example in Ref. 21.

The paper is organized as follows. In Section II we present a physical model able to capture the CS propagation on a surface of a 3D TI. Next, in Section III, we solve this physical model and derive the CS intensity. Its behavior is explored in Section IV for the case when the helical particle exciting the CS is oriented along the  $x$ -axis. Section V generalizes the results of Section IV and shows results for different orientations of the helical particle exciting the CS. The experimental relevance of the results is discussed in Section VI.

## II. PHYSICAL MODEL

As an application of our theory to a real physical setup, we will have in mind helical particles on a surface of  $\text{Bi}_2\text{Te}_3$ . Additionally, we will neglect possible sources of the particle-hole asymmetry. In this case the Hamiltonian of helical particles has the following form<sup>9</sup>:

$$\hat{H} = v(\hat{p}_x \hat{\sigma}_y - \hat{p}_y \hat{\sigma}_x) + \frac{\lambda}{2}(\hat{p}_+^3 + \hat{p}_-^3) \hat{\sigma}_z, \quad (1)$$

where  $\hat{p}_i$  and  $\hat{\sigma}_i$  ( $i = x, y$ ) are the momentum and spin-1/2 Pauli operators, respectively,  $\hat{p}_\pm \equiv \hat{p}_x \pm i\hat{p}_y$ . In Eq. (1) the first term describes the isotropic Dirac cone characterized by the velocity  $v$  while the second term describes the reduction of the full rotational symmetry down to the discrete threefold rotational symmetry. The strength of this anisotropic term is characterized by the parameter  $\lambda$ . For  $\text{Bi}_2\text{Te}_3$  the values of  $v$  and  $\lambda$  are given in Ref. 9,  $v = 3.87 \times 10^5$  m/s,  $\hbar^3 \lambda = 250.0$  eV  $\cdot \text{\AA}^3$ .

The Hamiltonian in Eq. (1) is easily diagonalized<sup>11</sup> and the resulting single-particle eigenenergies and eigen-

states are

$$\epsilon_{\mathbf{p}\mu} = \mu \sqrt{v^2 |\mathbf{p}|^2 + \lambda^2 |\mathbf{p}|^6 \cos^2(3\Theta_{\mathbf{p}})}, \quad (2)$$

$$\varphi_{\mathbf{p}\mu} = \begin{pmatrix} \cos(\alpha_{\mathbf{p}\mu}) \\ \mu i e^{i\Theta_{\mathbf{p}}} \sin(\gamma_{\mathbf{p}\mu}) \end{pmatrix}, \quad (3)$$

where  $\mu = \pm$  and  $\Theta_{\mathbf{p}}$  is the angle between the momentum  $\mathbf{p}$  and the  $x$ -axis,  $\alpha_{\mathbf{p}\mu} \equiv (1 - \mu)\pi/4 - \beta_{\mathbf{p}}$ ,  $\gamma_{\mathbf{p}\mu} \equiv (1 - \mu)\pi/4 + \beta_{\mathbf{p}}$ ,  $\sin(\beta_{\mathbf{p}}) = \sqrt{r(\mathbf{p})/[1 + r(\mathbf{p})]}$ , and  $\cos(\beta_{\mathbf{p}}) = 1/\sqrt{1 + r(\mathbf{p})}$

$$r(\mathbf{p}) = \frac{\sqrt{v^2 p^2 + \lambda^2 p^6 \cos^2(3\Theta_{\mathbf{p}})} - \lambda p^3 \cos(3\Theta_{\mathbf{p}})}{\sqrt{v^2 p^2 + \lambda^2 p^6 \cos^2(3\Theta_{\mathbf{p}})} + \lambda p^3 \cos(3\Theta_{\mathbf{p}})}. \quad (4)$$

The second quantized phonon Hamiltonian<sup>22</sup> is  $\hat{H}_{\text{ph}} = \sum_{\mathbf{k}} \hbar \omega(\mathbf{k}) (b_{\mathbf{k}}^\dagger b_{\mathbf{k}} + 1/2)$ , where  $b_{\mathbf{k}}^\dagger$ ,  $b_{\mathbf{k}}$  are the phonon creation and annihilation operators, respectively. We consider acoustic phonons and assume the following phonon spectrum  $\hbar \omega(\mathbf{k}) = c|\mathbf{k}|$  where  $c$  is the sound velocity. In principle in  $\text{Bi}_2\text{Te}_3$  there are longitudinal and transverse acoustic phonons with the corresponding sound velocities,  $c_l = 2.84 \times 10^3$  m/s,  $c_t = 1.59 \times 10^3$  m/s. However, for simplicity, we will assume the isotropic Debye model with  $c = c_l$ .

The helical electrons on a surface of a TI can excite sound. This happens via electron-phonon interaction. Due to this interaction the medium can emit phonons at any temperature. To explore the basic features of the CS we use the following Hamiltonian of the electron-phonon interaction<sup>23</sup>,

$$\begin{aligned} \hat{H}_{\text{el-ph}} &= g \sum_{\sigma} \int d\mathbf{r} \hat{\psi}_{\sigma}^{\dagger}(\mathbf{r}) \hat{\psi}_{\sigma}(\mathbf{r}) \hat{\varphi}(\mathbf{r}), \\ \hat{\varphi}(\mathbf{r}) &= i \sum_{\mathbf{k}} \sqrt{\frac{\hbar \omega(\mathbf{k})}{2V}} \left[ \exp\left(i \frac{\mathbf{k}\mathbf{r}}{\hbar}\right) b_{\mathbf{k}} - h.c. \right], \end{aligned} \quad (5)$$

where  $g$  is the strength of the electron-phonon interaction,  $V$  is the volume and  $\hat{\psi}_{\sigma}^{\dagger}(\mathbf{r})$ ,  $\hat{\psi}_{\sigma}(\mathbf{r})$  are, respectively, the helical particle creation and annihilation field operators.

## III. DERIVATION OF THE SOUND INTENSITY

The specific nature of the CS on a surface of a 3D TI is rooted in the properties of the eigenenergies (2) and eigenstates (3) of the Hamiltonian (1) describing the helical particles.

Using  $\epsilon_{\mathbf{p}\mu}$  and  $\varphi_{\mathbf{p}\mu}$  as well as the rules for the analytic reading<sup>23</sup> of Feynman diagrams, one may write down the analytic expression corresponding to the second order (in the strength  $g$  of the interaction between helical particles and phonons) diagram, Fig. 1, for the self-energy of a

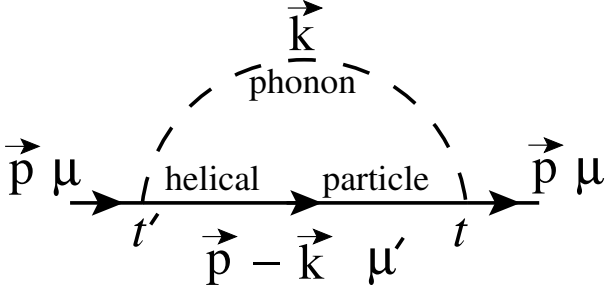


FIG. 1. Feynman diagram for the second-order contribution to the helical particle self-energy due to its interaction with phonons.

helical particle:

$$\begin{aligned} \Sigma_\mu(\mathbf{p}, t - t') &= \\ &= \frac{g^2}{\hbar} \sum_{\mu'} \int \frac{d\mathbf{k}}{(2\pi\hbar)^2} iG_{0\mu'}(\mathbf{p} - \mathbf{k}, t - t') \times \\ &\times D_0(\mathbf{k}, t - t') \Phi_{\mu\mu'}(\mathbf{p}, \mathbf{k}), \end{aligned} \quad (6)$$

where  $G_{0\mu}(\mathbf{p}, t - t')$  is the free propagator for a helical particle with momentum  $\mathbf{p}$  and chirality  $\mu$  and  $D_0(\mathbf{k}, t - t')$  is the free phonon propagator for a phonon with momentum  $\mathbf{k}$ . In the frequency domain these propagators have the form:

$$\begin{aligned} G_{0\mu}(\mathbf{p}, \omega) &= \frac{\hbar}{\hbar\omega - \epsilon_{\mathbf{p}\mu} + i \cdot 0} \\ D_0(\mathbf{k}, \omega) &= \frac{\omega^2(\mathbf{k})}{\omega^2 - \omega^2(\mathbf{k}) + i \cdot 0}. \end{aligned} \quad (7)$$

In Eq. (6) the quantity  $\Phi_{\mu\mu'}(\mathbf{p}, \mathbf{k})$  has the form:

$$\begin{aligned} \Phi_{\mu\mu'}(\mathbf{p}, \mathbf{k}) &= \cos^2(\alpha_{\mathbf{p}\mu}) \cos^2(\alpha_{\mathbf{p}-\mathbf{k}\mu'}) + \\ &+ \sin^2(\gamma_{\mathbf{p}\mu}) \sin^2(\gamma_{\mathbf{p}-\mathbf{k}\mu'}) + \\ &+ 2\mu\mu' \cos(\alpha_{\mathbf{p}\mu}) \cos(\alpha_{\mathbf{p}-\mathbf{k}\mu'}) \sin(\gamma_{\mathbf{p}\mu}) \sin(\gamma_{\mathbf{p}-\mathbf{k}\mu'}) \times \\ &\times \cos(\Theta_{\mathbf{p}-\mathbf{k}} - \Theta_{\mathbf{p}}). \end{aligned} \quad (8)$$

To get the sound intensity one has to transform Eq. (6) into the frequency domain, *i.e.*, to obtain  $\Sigma_\mu(\mathbf{p}, \omega)$  and then find its imaginary part on the mass surface, *i.e.*,  $\text{Im} \Sigma_\mu(\mathbf{p}, \omega)$  at  $\omega = \epsilon_{\mathbf{p}\mu}/\hbar$ .

As mentioned in the Introduction, the interchiral transitions do not contribute to the Cherenkov effect and thus it suffices to study the sound excited by helical particles with only one chirality. Choosing  $\mu = +$  (conduction band), we obtain

$$\begin{aligned} \text{Im} \Sigma_+(\mathbf{p}, \omega = \epsilon_{\mathbf{p}+}/\hbar) &= -\frac{g^2 c}{8\pi\hbar^3} \times \\ &\times \int_0^{k_D} dk \int_{-\pi}^{\pi} d\phi k^2 \Phi_{++}(\mathbf{p}, \mathbf{k}) \delta(\epsilon_{\mathbf{p}+} - \epsilon_{\mathbf{p}-\mathbf{k}+} - ck), \end{aligned} \quad (9)$$

where  $k_D$  is the Debye momentum.

Denoting the angle between the  $x$ -axis and the momentum of the helical particle, exciting CS, through  $\phi_0$  (*i.e.*,  $\Theta_{\mathbf{p}} = \phi_0$ ) and employing the formula

$$\delta[h(x)] = \sum_i \frac{1}{|h'(x_i)|} \delta(x - x_i), \quad (10)$$

where  $h'(x) \equiv d[h(x)]/dx$  and  $h(x_i) = 0$ , we finally obtain

$$\text{Im} \Sigma_+(\mathbf{p}, \omega = \epsilon_{\mathbf{p}+}/\hbar) = -\frac{g^2 p^2}{8\pi\hbar^3} \int_{-\pi}^{\pi} d\phi W(\phi). \quad (11)$$

Defining  $x \equiv k/p$  and taking into account that for a fixed momentum  $\mathbf{p}$  one has  $\Phi_{++}(\mathbf{p}, \mathbf{k}) = \Phi_{++}(x, \phi)$ , where  $\phi$  is the angle between  $\mathbf{p}$  and  $\mathbf{k}$ , the dimensionless sound intensity  $W(\phi)$  in Eq. (11) may be written as follows:

$$W(\phi) = \sum_i \frac{x_i^2(\phi) \Phi_{++}[x_i(\phi), \phi]}{|\chi'[x_i(\phi), \phi]|}, \quad (12)$$

where  $x_i(\phi)$  are the roots of the equation  $\Delta\varepsilon(x, \phi) \equiv \epsilon_{\mathbf{p}+} - \epsilon_{\mathbf{p}-\mathbf{k}+} - ck = 0$  accounting for the energy and momentum conservation in the system. It can be written as

$$\begin{aligned} \sqrt{a^2 + b^2 \cos^2(3\phi_0)} - \sqrt{a^2 \zeta(x, \phi) + b^2 \xi(x, \phi)} - \\ - x = 0, \end{aligned} \quad (13)$$

where

$$\begin{aligned} \zeta(x, \phi) &\equiv 1 + x^2 - 2x \cos(\phi), \\ \xi(x, \phi) &\equiv [\cos(\phi_0) - x \cos(\phi + \phi_0)]^2 \times \\ &\times [1 - 4 \sin^2(\phi_0) + x^2(4 \cos^2(\phi + \phi_0) - 3) - \\ &- 2x(4 \cos(\phi_0) \cos(\phi + \phi_0) - 3 \cos(\phi))]^2. \end{aligned} \quad (14)$$

The function  $\chi'(x, \phi)$  is defined as  $\chi'(x, \phi) \equiv \partial_x \chi(x, \phi)$ , where  $\chi(x, \phi) \equiv \Delta\varepsilon(x, \phi)/cp$ . The dimensionless parameters  $a$  and  $b$  characterize the ratio of the Dirac and sound velocities,  $a \equiv v/c$ , and the strength of the energy-momentum anisotropy,  $b \equiv \lambda p^2/c$ .

Let us discuss the physical meaning of the quantities in the expression for the sound intensity, Eq. (12).

The roots  $x_i(\phi)$  represent the phonon momenta allowed by the energy and momentum conservation. Physically it is clear that larger values of the allowed phonon momenta must result in larger values of the sound intensity. This is mathematically expressed by the fact that the square of the magnitude of the allowed phonon momenta is in the numerator of Eq. (12).

However, different roots  $x_i(\phi)$  have different physical significance. Indeed, imagine that the magnitude of a given allowed phonon momentum  $x_i(\phi)$  is infinitesimally shifted keeping the direction  $\phi$  of this momentum fixed. Then  $\Delta\varepsilon(x, \phi)$  will deviate from zero indicating a violation of the energy and momentum conservation, Eq. (13). For different  $x_i(\phi)$  this deviation has different rates. For a given  $x_i(\phi)$  a slower deviation from the conservation

laws gives evidence for its greater physical significance and thus this phonon momentum must bring a larger contribution to the sound intensity. Exactly this physical aspect is mathematically controlled by  $\chi'(x, \phi)$  in the denominator of Eq. (12). In particular, if there is another allowed phonon momentum infinitesimally close to  $x_i(\phi)$  then the energy and momentum conservation will not be violated at all and the corresponding contribution to the sound intensity will be very large.

To understand the physical meaning of  $\Phi_{++}(x, \phi)$  in Eq. (12) let us recall that the interaction between helical particles and phonons is diagonal in spin. It is, therefore, useful to consider an operator  $\hat{O}$  diagonal in spin,  $\langle \mathbf{p}'\sigma' | \hat{O} | \mathbf{p}\sigma \rangle = \delta_{\sigma\sigma'} O_{\mathbf{p}'\mathbf{p}}$ , and calculate its matrix elements between the eigenstates given by Eq. (3). One readily finds  $\langle \mathbf{p}'\mu' | \hat{O} | \mathbf{p}\mu \rangle = O_{\mathbf{p}'\mathbf{p}} w_{\mathbf{p}'\mu'\mathbf{p}\mu}$ , where

$$w_{\mathbf{p}'\mu'\mathbf{p}\mu} \equiv \cos(\alpha_{\mathbf{p}'\mu'}) \cos(\alpha_{\mathbf{p}\mu}) + \mu' \mu e^{i(\Theta_{\mathbf{p}} - \Theta_{\mathbf{p}'})} \sin(\gamma_{\mathbf{p}'\mu'}) \sin(\gamma_{\mathbf{p}\mu}). \quad (15)$$

The quantity  $|w_{\mathbf{p}'\mu'\mathbf{p}\mu}|^2$  determines the quantum mechanical probability of the transition  $\varphi_{\mathbf{p}\mu} \rightarrow \varphi_{\mathbf{p}'\mu'}$  induced by the perturbation  $\hat{O}$ . It is easy to see that  $\Phi_{\mu\mu'}(\mathbf{p}, \mathbf{k}) = |w_{\mathbf{p}-\mathbf{k}\mu'\mathbf{p}\mu}|^2$ . Therefore, the physical meaning of  $\Phi_{++}(x, \phi)$  in Eq. (12) is the quantum mechanical probability for a helical particle to scatter within the conduction band ( $\mu = +$ ) from momentum  $\mathbf{p}$  to momentum  $\mathbf{p} - \mathbf{k}$ , where the angle between  $\mathbf{p}$  and  $\mathbf{k}$  is equal to  $\phi$  and  $k = px$ . Equivalently, this probability may be called phonon emission probability. It is physically clear that the phonons whose emission probability is higher will produce larger contributions to the sound intensity. Mathematically this is expressed by the fact that  $\Phi_{++}(x, \phi)$  enters the numerator of Eq. (12).

Finally, Fig. 2 explains the physical origin of the anomalous CS. As one can see, the reason for this sound is the anisotropy of the constant energy surfaces. In the isotropic case an emitted phonon (with the energy  $\varepsilon - \varepsilon'$ ) always has its momentum  $\mathbf{k}$  with a forward orientation,  $\phi < \pi/2$ . However, when the anisotropy becomes strong enough, it admits phonons with orientations  $\phi = \pi/2$  as well as  $\phi > \pi/2$ .

#### IV. RESULTS FOR CS EXCITED BY HELICAL PARTICLES WITH $\phi_0 = 0$

All specific features of the CS on a surface of a 3D TI, mentioned in the Introduction, may already be observed when the helical particle, exciting the CS, is oriented along the  $x$ -axis,  $\phi_0 = 0$ . Therefore in this section we consider this specific case in detail. The generalization to  $\phi_0 \neq 0$  is given in the next section.

The angular distribution of the CS intensity for not too large values of the anisotropy parameter  $b$  is shown in Fig. 3. When the anisotropy increases there appears a plateau at small angles and sharp peaks on the surface of the Cherenkov cone  $\phi = \pm\phi_c \approx \pm\pi/2$ . Physically, this

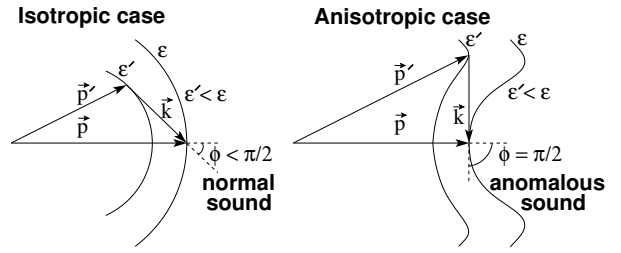


FIG. 2. The schematic picture of the transition processes allowed by the energy and momentum conservation. Here  $\varepsilon$  and  $\mathbf{p}$  are the energy and momentum of a helical particle before its scattering while  $\varepsilon'$  and  $\mathbf{p}'$  are the energy and momentum of this helical particle after its scattering. The momentum of the emitted phonon is denoted through  $\mathbf{k}$ .

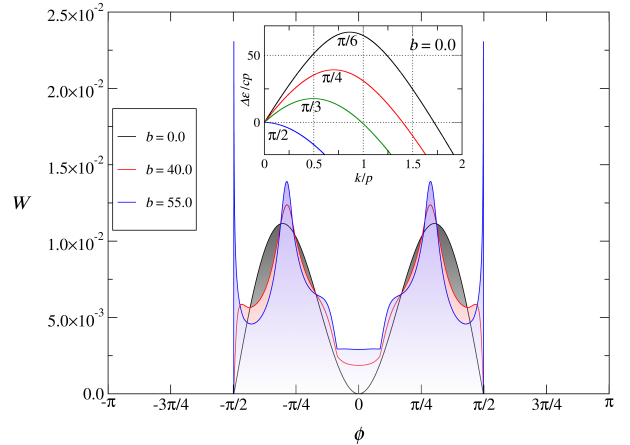


FIG. 3. (Color online) The CS intensity (excited by a helical particle moving along the  $x$ -axis) as a function of  $\phi$  for several values of  $b$ . For  $\text{Bi}_2\text{Te}_3$   $a = 136.3$ . Inset:  $\Delta\varepsilon/cp$  as a function of  $k/p$  for different angles  $\phi$  and  $b = 0$ .

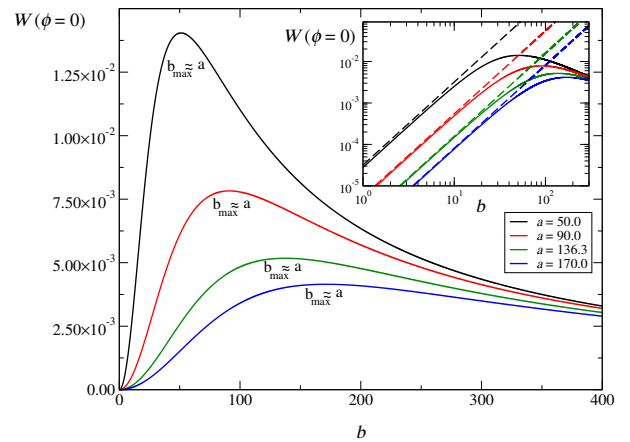


FIG. 4. (Color online) The intensity of the strictly forward CS as a function of the anisotropy strength  $b$  for several values of the parameter  $a$ . The inset shows the expected power law behavior (which is linear in the log-log scale) at small  $b$ .

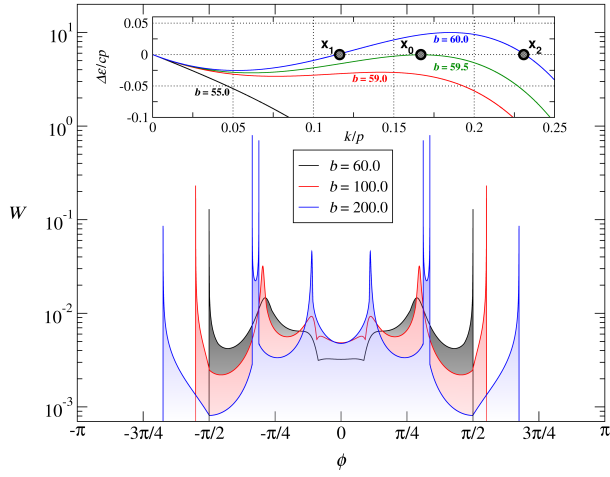


FIG. 5. (Color online) The angular distribution of the CS intensity for stronger anisotropy  $b$ . Here  $a = 136.3$ . Inset:  $\Delta\varepsilon/cp$  as a function of  $k/p$  at  $\phi = \phi_c$  and  $b = 55.0$  (black),  $b = 59.0$  (red),  $b = 59.5$  (green) and  $b = 60.0$  (blue).

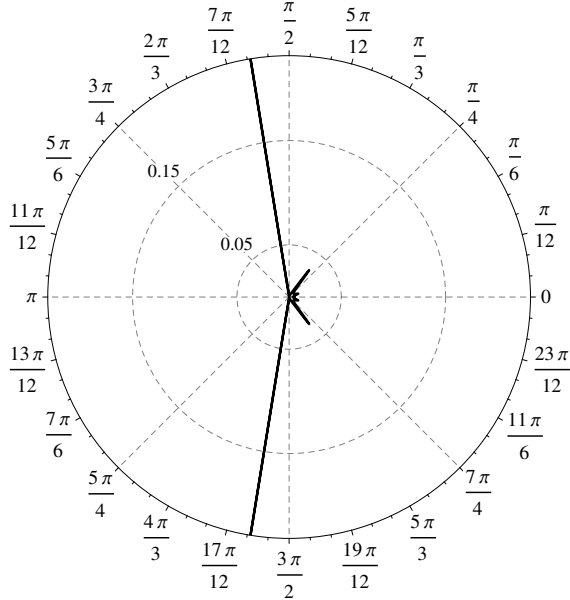


FIG. 6. The 2D distribution of the CS on a surface of a TI for  $a = 136.3$  and  $b = 100.0$ .

behavior can be explained in terms of the quantum mechanical probability of a phonon emission and the energy and momentum conservation (see the previous section). When the angle increases from zero to a small finite value, the phonon emission probability, obtained from Eq. (15), decreases. But phonon momenta with finite angles bring larger contributions to the sound intensity. As explained in Section III, for these momenta the violation of the energy and momentum conservation (when infinitesimally shifting their magnitudes and keeping their orientations unchanged) becomes much weaker when the angle grows (this fact is mathematically controlled by the denomi-

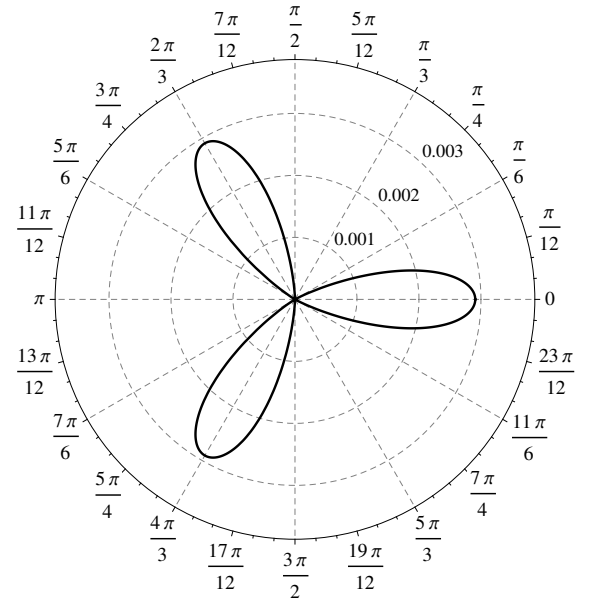


FIG. 7. The strictly forward CS as a function of the momentum orientation  $\phi_0$  of the helical particle exciting the sound. Here  $a = 136.3$  and  $b = 55.0$ .

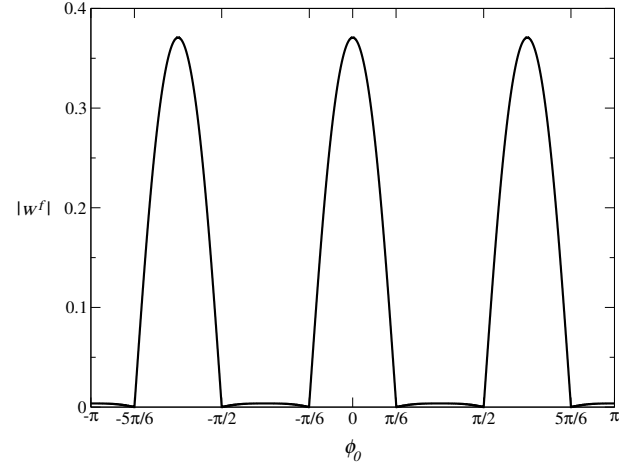


FIG. 8. The quantum mechanical transition probability for the case of the strictly forward CS as a function of the momentum orientation  $\phi_0$  of the helical particle exciting this sound. Here  $a = 136.3$  and  $b = 55.0$ .

nator in Eq. (12)). This compensates the decrease of the emission probability leading to a plateau. At angles close to  $\phi_c$  a finite momentum, allowed by the energy and momentum conservation, approaches the zero momentum (also allowed). Therefore, an infinitesimal shift of its magnitude has a little impact on the energy and momentum conservation. Thus this phonon momentum brings a very large contribution to the sound intensity. At the same time its magnitude approaches zero. This results in a sharp maximum in the vicinity of  $\phi_c$ .

The inset explains, for the case  $b = 0$ , the mechanism of the disappearance of the CS outside the Cherenkov

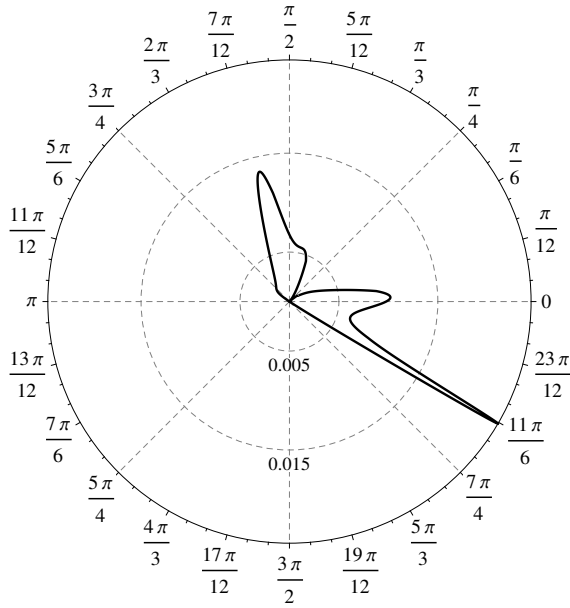


FIG. 9. The intensity of the CS as a function of  $\phi + \phi_0$ , where  $\phi_0$  is the orientation of the helical particle exciting the sound, *i.e.*, the orientation of  $\mathbf{p}$ , while  $\phi$  is the angle between  $\mathbf{p}$  and the direction of the excited sound, *i.e.*, the angle between  $\mathbf{p}$  and  $\mathbf{k}$ . Here  $\phi_0 = \pi/4$ ,  $a = 136.3$  and  $b = 55.0$ .

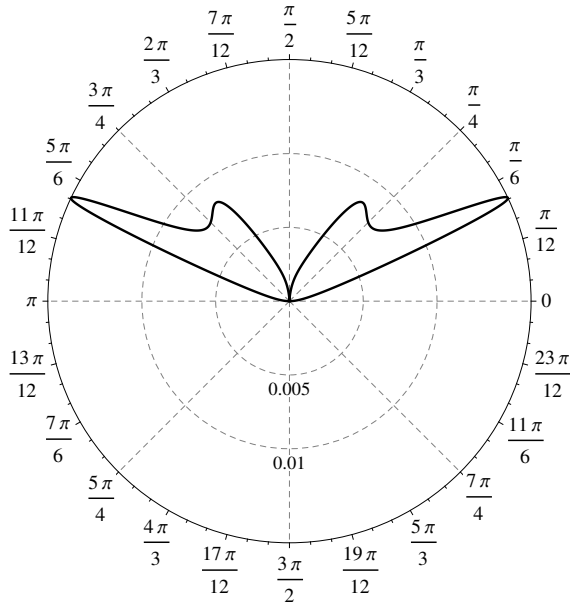


FIG. 10. The same as in Fig. 9, but for  $\phi_0 = \pi/2$ .

cone: at angles  $|\phi| < \phi_c$  the equation  $\Delta\varepsilon/cp = 0$  has one finite root  $k/p$  which merges with the zero root as soon as the angle approaches the critical value  $\phi_c$ . A similar mechanism underlies the angular distribution of the sound intensity for the case  $b \neq 0$ : there still exists only one finite root which merges with zero when  $\phi$  approaches  $\phi_c$  but the larger  $b$  is the slower this merging becomes. Physically, the restriction of the sound to the

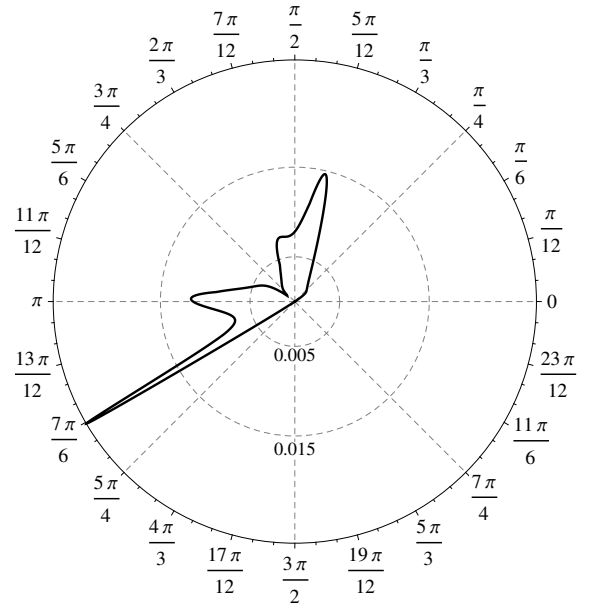


FIG. 11. The same as in Fig. 9, but for  $\phi_0 = 3\pi/4$ .

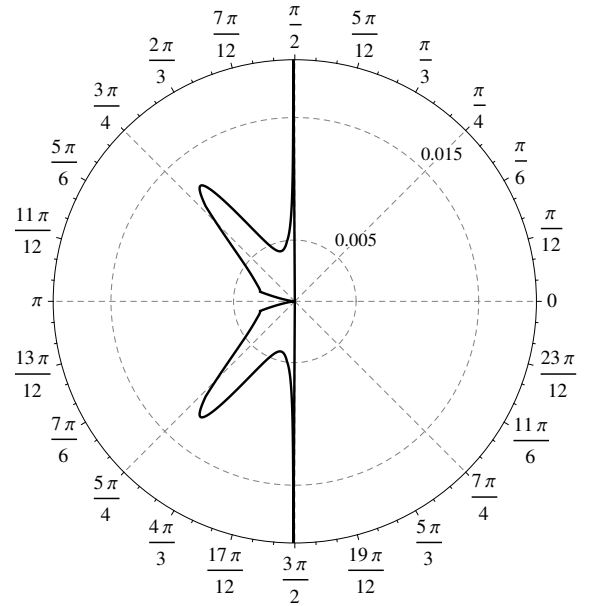


FIG. 12. The same as in Fig. 9, but for  $\phi_0 = \pi$ .

cone can be seen from the energy and momentum conservation. The energy of the helical particle exciting the CS decreases. For weak anisotropy the constant energy surfaces are almost circles. Thus the helical particle moves from a circle with a larger radius to a circle with a smaller radius. This can only lead to excitation of forward sound (see Fig. 2).

In Fig. 4 a new feature of the CS on a surface of a 3D TI, strictly forward sound, is shown in detail. To demonstrate its properties we plot it as a function of the anisotropy for different ratios of the Dirac and sound ve-

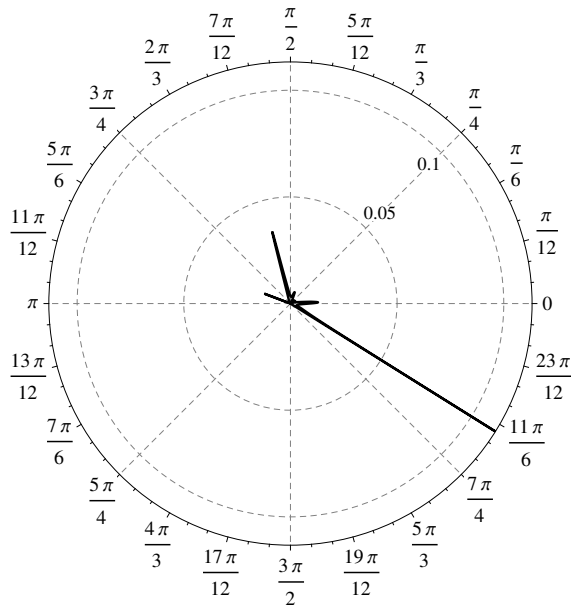


FIG. 13. The same as in Fig. 9, but for  $\phi_0 = \pi/4$  and  $b = 100$ .

locities. All the curves have a maximum at a certain value  $b_{\max}$ . Our results clearly show that  $b_{\max} \approx a$ . This is an important issue for experiments since it implies the ratio  $v = \lambda p^2$ . This ratio shows that if the momentum  $p$  of the helical electron, exciting the CS, is known, then the anisotropy parameter  $\lambda$  can easily be obtained. This is experimentally relevant because electrons exciting the sound may be prepared with a definite momentum before they hit the surface. Another aspect of the strictly forward sound is that at zero anisotropy it vanishes. The inset compares this vanishing behavior with the exact asymptotics  $W(\phi = 0) = 4b^2/a^3 = 4\lambda^2 p^4 c/v^3$  which offers an alternative possibility to measure the anisotropy at small momenta  $p$  of incident electrons.

The nature of the CS on a surface of a 3D TI acquires another fundamental change when the anisotropy becomes strong as it is shown in Fig. 5. As soon as the anisotropy exceeds a critical value  $b_c = 59.5$ , the CS overcomes the critical angle  $\phi_c \approx \pi/2$  and starts to propagate in backward directions, *i.e.*, there appears the anomalous CS. The inset explains the mechanism responsible for the formation of the anomalous CS. At  $\phi = \phi_c$  and  $b < b_c$  the equation  $\Delta\varepsilon/cp = 0$  has no finite roots  $k/p$  and thus the sound intensity is zero. However, at  $b = b_c$  a single finite root appears giving a finite contribution to the sound intensity. This leads to a jump from zero to a finite value of the sound intensity on the surface of the Cherenkov cone  $\phi = \phi_c$ . Further this root splits into two finite roots which both bring finite contributions to the anomalous CS. The physical explanation of the anomalous CS is again given by the energy and momentum conservation. The helical particle exciting the CS moves from a constant energy surface with a larger energy to a constant energy surface with a smaller energy. At the

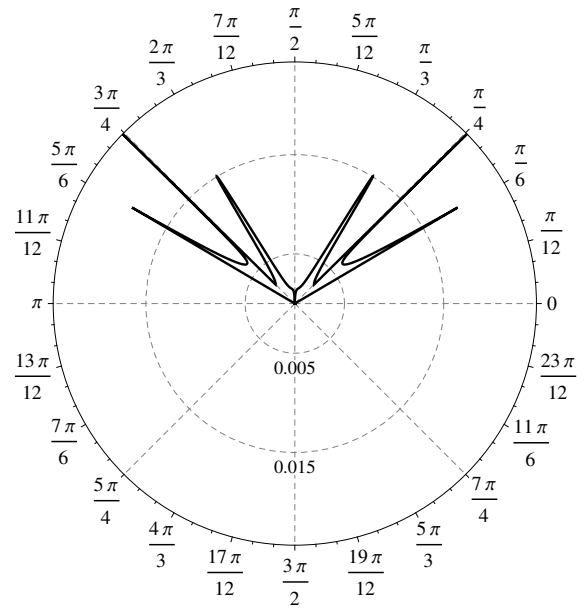


FIG. 14. The same as in Fig. 9, but for  $\phi_0 = \pi/2$  and  $b = 200$ .

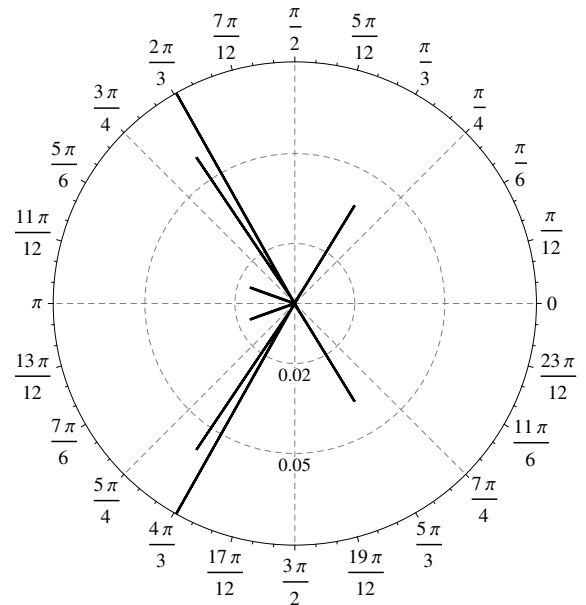


FIG. 15. The same as in Fig. 9, but for  $\phi_0 = \pi$  and  $b = 200$ .

same time for strong anisotropy the constant energy surfaces acquire a negative curvature. Exactly this negative curvature admits the anomalous CS (see Fig. 2).

The 2D distribution of the CS on a surface of a TI in the regime of strong anisotropy is shown in Fig. 6 for  $b = 100.0$ . As one can see, in this regime the CS intensity is mainly located along specific forward and backward directions. In other words, the CS localizes into a few normal and anomalous beams. The physical reason for the localization of the CS at discrete angles is that at these angles the violation of the energy and momentum con-

servation (see the previous section) becomes very weak because in the vicinities of these angles the curvature of the constant energy surfaces becomes minimal. In the regime of strong anisotropy the angular domains, where this curvature is minimal, become extremely narrow and, as a result, large values of the sound intensity are located in very small areas around discrete angles.

## V. RESULTS FOR CS EXCITED BY HELICAL PARTICLES WITH $\phi_0 \neq 0$

Here we show some results for the CS excited by helical particles whose momentum orientation differs from the one of the  $x$ -axis, that is by helical particles with  $\phi_0 \neq 0$ .

The results of Section III are valid for any angle  $\phi_0$  and the sound intensity can be obtained from Eq. (12).

In particular, one can obtain the strictly forward sound as a function of  $\phi_0$ . It is shown in Fig. 7 using polar coordinates for the anisotropy strength  $b = 55.0$  (here and below  $a = 136.3$  which is the value for  $\text{Bi}_2\text{Te}_3$ ). As one can see, the intensity of the strictly forward sound has the discrete threefold rotational symmetry of the helical particle Hamiltonian, Eq. (1). The specific feature of the strictly forward sound is that it is enhanced in the sectors  $(-\pi/6, \pi/6)$ ,  $(\pi/2, 5\pi/6)$  and  $(-5\pi/6, -\pi/2)$  but suppressed outside them. At the angles  $\phi_0 = \pm\pi/6, \pm5\pi/6, \pm\pi/2$  the strictly forward sound vanishes because at these values the anisotropy has no effect, as one can see from Eqs. (2) and (4). The enhancement and suppression of the strictly forward sound can be explained by the behavior of the quantum mechanical transition probability which is determined by  $w_{\mathbf{p}'\mu'\mathbf{p}\mu}$ , Eq. (15). In the case of the strictly forward phonon emission it takes the form  $w^f(\mathbf{p}, \mathbf{k}) = \cos(\beta_{\mathbf{p}-\mathbf{k}})\cos(\beta_{\mathbf{p}}) \pm \sin(\beta_{\mathbf{p}-\mathbf{k}})\sin(\beta_{\mathbf{p}})$ , where the sum is taken for  $x < 1$  ( $k < p$ ) and the difference is taken for  $x > 1$  ( $k > p$ ). From this expression it is also easy to see that in the absence of the anisotropy,  $b = 0$ ,  $w^f(\mathbf{p}, \mathbf{k}) = 0$ . Indeed, for  $b = 0$  and  $a \gg 1$  (which is our case because  $a = 136.3$ ) the only finite solution allowed by the energy and momentum conservation is  $x \approx 2 - 2/a$ . Therefore,  $x > 1$  and  $w^f(\mathbf{p}, \mathbf{k}) = \cos(\beta_{\mathbf{p}-\mathbf{k}})\cos(\beta_{\mathbf{p}}) - \sin(\beta_{\mathbf{p}-\mathbf{k}})\sin(\beta_{\mathbf{p}})$ . Since for  $b = 0$  we have  $\cos(\beta_{\mathbf{p}-\mathbf{k}}) = \cos(\beta_{\mathbf{p}}) = \sin(\beta_{\mathbf{p}-\mathbf{k}}) = \sin(\beta_{\mathbf{p}}) = 1/\sqrt{2}$ , we conclude that  $w^f(\mathbf{p}, \mathbf{k}) = 0$ . Therefore, the reason for nonzero strictly forward sound is the anisotropic nature of the helical states. At finite anisotropy,  $b = 55.0$ , the absolute value  $|w^f(\mathbf{p}, \mathbf{k})|$  is shown in Fig. 8 as a function of  $\phi_0$ . It has large values in the sectors  $(-\pi/6, \pi/6)$ ,  $(\pi/2, 5\pi/6)$  and  $(-5\pi/6, -\pi/2)$  and it is very small outside them. This nicely explains the specific dependence of the strictly forward sound shown in Fig. 7.

Finally, we show the angular distribution of the CS intensity on a surface of a 3D TI for different orientations of the helical particle exciting the sound, *i.e.*, for different values of  $\phi_0$  as well as for different levels of the anisotropy, *i.e.*, for different values of  $b$ .

In Fig. 9 the CS intensity is shown for  $\phi_0 = \pi/4$  and  $b = 55.0$ . The characteristic feature of the sound distribution in this case is its asymmetry with respect to the orientation of the helical particle, *i.e.*, with respect to  $\mathbf{p}$ . The symmetry of the sound distribution is restored when  $\mathbf{p}$  approaches an orientation with respect to which the constant energy surfaces have a certain symmetry as it happens, *e.g.*, in the case  $\phi_0 = \pi/2$  shown in Fig. 10. Increasing  $\phi_0$  further again leads to a loss of the symmetry of the sound distribution, shown in Fig. 11 for  $\phi_0 = 3\pi/4$ . Another recovery of the symmetry takes place at  $\phi_0 = \pi$ , Fig. 12.

In the previous section it has been shown that at strong anisotropy a helical particle moving along the  $x$ -axis,  $\phi_0 = 0$ , excites the CS propagating mainly along specific directions, *i.e.*, the CS localizes into a few forward and backward beams. Here we show that this specific feature of the CS on a surface of a 3D TI is retained when the particle exciting the sound moves along an arbitrary direction  $\phi_0 \neq 0$ . Indeed, Fig. 13 shows for the case  $\phi_0 = \pi/4$  and  $b = 100$  that the sound is mainly located within four forward beams and one backward beam. Fig. 14 demonstrates that in the case  $\phi_0 = \pi/2$ ,  $b = 200$  there are only six forward beams, which are a bit delocalized, while for  $\phi_0 = \pi$ ,  $b = 200$  Fig. 15 illustrates a strong localization of the CS into eight beams, six forward and two backward ones.

## VI. CONCLUSIONS

In conclusion, let us estimate the relevance of our results for experiments. In the regime of strong anisotropy, *e.g.*, at  $b = 200.0$ , one gets  $p \approx 1.28 \cdot 10^{-25}$  kg·m/s. In terms of the corresponding wave vector,  $p = \hbar q$ , one has  $q \approx 0.12\text{\AA}^{-1}$  which is well within the modern experiments<sup>9</sup>. Further, the analysis above has been performed at zero temperature. At finite temperature  $T$  there will appear a noninteracting (or ideal) phonon gas. The average energy of a phonon in this gas is of order  $k_B T$ . As soon as the energy of the phonons in the CS exceeds  $k_B T$ , the sound distribution will not be affected by thermal phonons. Since  $k \sim 2p$  (see the previous section) and for  $b = 200.0$  we have  $p \approx 1.28 \cdot 10^{-25}$  kg·m/s, we get from the condition  $k_B T_0 = ck$  that for temperatures  $T < T_0 \approx 53\text{K}$  the CS will not be affected by thermal phonons. At higher temperatures the sharp Cherenkov peaks shown in Fig. 5 should start to wash out. Finally, our assumption of the isotropic Debye model has a little effect on the results presented above. First, for  $\text{Bi}_2\text{Te}_3$  the Debye wave vector is  $k_D \approx 1.3\text{\AA}^{-1}$ , *i.e.*, it is much above the magnitudes of the phonon wave vectors in the CS. Second, the phonon anisotropy,  $c_l/c_t \approx 1.8$ , is much weaker than the CS anisotropy (several orders of magnitude). Therefore, the contribution of the phonon anisotropy to the total anisotropy of the CS will be negligible.

The estimate above clearly demonstrates that the CS

on a surface of a 3D TI and its unique features explored here may really be accessed and utilized in modern experiments and future electronic devices based on 3D TI. Another aspect making the CS fundamentally important is dissipation unavoidable in realistic devices coupled to external environments. The CS is a ubiquitous dissipative mechanism which, as follows from our estimate above, may determine the efficiency of electronic devices based

on helical particles.

## VII. ACKNOWLEDGMENTS

Support from the DFG under the program SFB 689 is acknowledged.

- 
- <sup>1</sup> M. Z. Hasan and C. L. Kane, *Rev. Mod. Phys.* **82**, 3045 (2010).
- <sup>2</sup> X.-L. Qi and S.-C. Zhang, *Rev. Mod. Phys.* **83**, 1057 (2011).
- <sup>3</sup> C. Wu, B. A. Bernevig, and S.-C. Zhang, *Phys. Rev. Lett.* **96**, 106401 (2006).
- <sup>4</sup> C. Xu and J. E. Moore, *Phys. Rev. B* **73**, 045322 (2006).
- <sup>5</sup> M. König, S. Wiedmann, C. Brune, A. Roth, H. Buhmann, L. W. Molenkamp, X.-L. Qi, and S.-C. Zhang, *Science* **318**, 766 (2007).
- <sup>6</sup> A. Roth, C. Brune, H. Buhmann, L. W. Molenkamp, J. Maciejko, X.-L. Qi, and S.-C. Zhang, *Science* **325**, 294 (2009).
- <sup>7</sup> H. Zhang, C.-X. Liu, X.-L. Qi, X. Dai, Z. Fang, and S.-C. Zhang, *Nature Physics* **5**, 438 (2009).
- <sup>8</sup> Y. L. Chen, J. G. Analytis, J.-H. Chu, Z. K. Liu, S.-K. Mo, X. L. Qi, H. J. Zhang, D. H. Lu, X. Dai, Z. Fang, S. C. Zhang, I. R. Fisher, Z. Hussain, and Z.-X. Shen, *Science* **325**, 178 (2009).
- <sup>9</sup> L. Fu, *Phys. Rev. Lett.* **103**, 266801 (2009).
- <sup>10</sup> C.-X. Liu, X.-L. Qi, H. Zhang, X. Dai, Z. Fang, and S.-C. Zhang, *Phys. Rev. B* **82**, 045122 (2010).
- <sup>11</sup> C. M. Wang and F. J. Yu, *Phys. Rev. B* **84**, 155440 (2011).
- <sup>12</sup> P. A. Cherenkov, *Doklady Akad. Nauk SSSR* **2**, 451 (1934).
- <sup>13</sup> I. E. Tamm and I. M. Frank, *Doklady Akad. Nauk. SSSR* **14**, 107 (1937).
- <sup>14</sup> L. D. Landau and E. M. Lifshitz, *Electrodynamics of Continuous Media: Course of Theoretical Physics*, Vol. 8 (Butterworth-Heinemann, Oxford, UK, 1984).
- <sup>15</sup> L. S. Levitov and A. V. Shitov, *Green's Functions. Problems and Solutions*, 2nd ed. (Fizmatlit, Moscow, 2003) in Russian.
- <sup>16</sup> S. Smirnov, *Phys. Rev. B* **83**, 081308(R) (2011).
- <sup>17</sup> Y. A. Bychkov and E. I. Rashba, *JETP Letters* **39**, 78 (1984).
- <sup>18</sup> S. M. Komirenko, K. W. Kim, A. A. Demidenko, V. A. Kochelap, and M. A. Stroschio, *Appl. Phys. Lett.* **76**, 1869 (2000).
- <sup>19</sup> X. F. Zhao, J. Zhang, S. M. Chen, and W. Xu, *J. Appl. Phys.* **105**, 104514 (2009).
- <sup>20</sup> C. Luo, M. Ibanescu, S. G. Johnson, and J. D. Joannopoulos, *Science* **299**, 368 (2003).
- <sup>21</sup> C. X. Zhao, W. Xu, and F. M. Peeters, *Appl. Phys. Lett.* **102**, 222101 (2013).
- <sup>22</sup> L. D. Landau and E. M. Lifshitz, *Statistical Physics. Part 1: Course of Theoretical Physics*, Vol. 5 (Pergamon Press, 1980).
- <sup>23</sup> A. A. Abrikosov, L. P. Gorkov, and I. E. Dzyaloshinski, *Methods of Quantum Field Theory in Statistical Physics* (Dover, New York, 1963).